Investigating human monocyte adhesion, migration and transmigration and their modulation by Zika virus

Emma Partiot, Diana Brychka, Raphael Gaudin

European Journal of Cell Biology 103 (2024) 151453

Contents lists available at ScienceDirect

European Journal of Cell Biology

journal homepage: www.elsevier.com/locate/ejcb

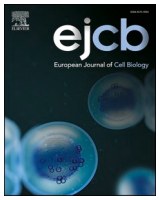

Short communication

Investigating human monocyte adhesion, migration and transmigration and their modulation by Zika virus

Emma Partiot [a,b], Diana Brychka [a,b], Raphael Gaudin [a,b,*]

[a] CNRS, Institut de Recherche en Infectiologie de Montpellier (IRIM), Montpellier 34293, France
[b] Univ Montpellier, Montpellier 34090, France

ARTICLE INFO

Keywords:
Flavivirus
Neuroinvasion
Cytoskeleton
Actin
Rho GTPase
Endothelium

ABSTRACT

Human circulating monocytes are established targets for Zika virus (ZIKV) infection. Because of their important migratory properties toward any tissues, including the central nervous system (CNS), a better understanding of the mechanisms underlying monocyte transmigration upon ZIKV infection is required. Here, we monitored adhesion, migration and transmigration properties of monocytes exposed to ZIKV. We found that ZIKV enhanced monocyte adhesion on collagen compared to mock-exposed samples, and that pharmacological inhibition of mDia and Cdc42 function induced a significant decrease of adhesion in both mock- and ZIKV-exposed monocytes. In contrast, monocyte migration through collagen was inhibited by most of the tested small molecules targeting regulators of actin polymerization, including Rac1, ROCK, Cdc42, mDia, Arp2/3, Myosin-II and LFA-1. ZIKV-exposed monocyte migration showed a very similar profile to that of their mock-exposed counterparts. Finally, assessment of monocyte transmigration through human cerebral microvascular endothelial cells (hCMEC/D3) showed dependency on Rac1, ROCK, and Cdc42, independently of their infection status. In contrast, we identified that BIRT377, an antagonist of LFA-1, significantly inhibited transmigration of ZIKV-exposed but not mock-exposed monocytes. As BIRT377 increased adhesion of ZIKV-exposed monocytes, we propose that LFA-1 might be involved in a post-adhesion step to enhance viro-induced transmigration. These data suggest that ZIKV exposure triggers specific migratory properties of monocytes that are not exploited under physiological conditions. This work provides further insights on virus-host interactions important for viral neuroinvasion and offers novel targets to specifically inhibit the infiltration of infected cells to the CNS.

Summary sentence: Monocyte transmigration involves massive actin cytoskeleton reorganization regulated by small Rho GTPases and integrins, which can be subverted by viruses.

1. Introduction

Zika virus (ZIKV) is a public health concern worldwide (Lessler et al., 2016) for which no approved vaccine or drugs are currently available. ZIKV is a blood-borne pathogen from the *Flaviviridae* family that is transmitted through the bite of an infected mosquito from the *Aedes* genus, mainly *Aedes aegypti*. The most severe complications include fetal microcephaly in pregnant women, as well as other neurological disorders in fetuses, but also in newborns, infants and adults, including Guillain-Barré syndrome and altered functional connectivity between brain areas involved in social and emotional behaviors (Lessler et al., 2016; Li et al., 2016a; Baud et al., 2017; Pierson and Diamond, 2018; Mavigner et al., 2018; Raper et al., 2020). The wide dissemination of the virus within the body suggests that molecular and cellular mechanisms from the host are subverted to allow ZIKV virions to travel from their entry site toward tissues. This is particularly important for the difficult-to-access brain sanctuary. ZIKV efficiently invades and persists within the brain (Aid et al., 2017; Hirsch et al., 2017; Bhatnagar et al., 2017) and exhibits a preferential tropism for human neural progenitor cells (hNPCs), which are key players in the development of ZIKV-induced neurological disease (Li et al., 2016a, 2016a; Yockey et al., 2016; Tang et al., 2016).

To be protected and reach remote tissues, viruses can hide inside cells from the bloodstream and be transported through the blood-brain barrier (BBB), a phenomenon referred to as the Trojan Horse strategy, proposed over 35 years ago (Peluso et al., 1985). Several studies have previously shown that viruses, including ZIKV, exploit and enhance this pathway (Peluso et al., 1985; Li et al., 2016b; Laval et al., 2015; Paul

* Correspondence to: Institut de Recherche en Infectiologie de Montpellier (IRIM), Univ Montpellier, CNRS, Montpellier, France.
E-mail address: raphael.gaudin@irim.cnrs.fr (R. Gaudin).

https://doi.org/10.1016/j.ejcb.2024.151453
Received 5 April 2024; Received in revised form 25 July 2024; Accepted 18 August 2024
Available online 22 August 2024

et al., 2017; Tiong et al., 2018; Ayala-Nunez et al., 2019), but the underlying molecular mechanisms leading to increased cell migration have not been investigated in detail. We have previously shown that ZIKV induces the overexpression of several attachment factors at the surface of circulating human monocytes, leading to increased monocyte attachment and transmigration through endothelial cells *in vitro* and in zebrafish (Ayala-Nunez et al., 2019). It has also been previously reported using differential proteomic analysis that several integrins, focal adhesion (FA) and actin-related proteins were up-regulated in ZIKV-exposed monocytes.

Integrins and FA proteins are involved in several steps of the transmigration process. Indeed, depending on integrin expression at the surface, adhesion of the migratory cells to the endothelium would shift from light to firm adhesion. On the other hand, some integrins have also been described as involved in the diapedesis process by competing with tight junction interaction proteins of the monolayer (Ostermann et al., 2002; Weber et al., 2007). Integrin interaction with a ligand leads to a signalization cascade which results in integrin assembly and disassembly, a process in association with actin-binding proteins (Vicente-Manzanares et al., 2009).

In cells, actin dynamics are mainly regulated by Cdc42, Rac1 and RhoA, three highly conserved members of family of small Rho GTPases (Hall, 1998). Among them, Cdc42 and Rac1 are mostly involved in the regulation of cell protrusions, while RhoA is responsible for controlling cell contractility. Furthermore, virus targeting of Rho GTPases favors cell entry and replication (Van den Broeke et al., 2014). However, the

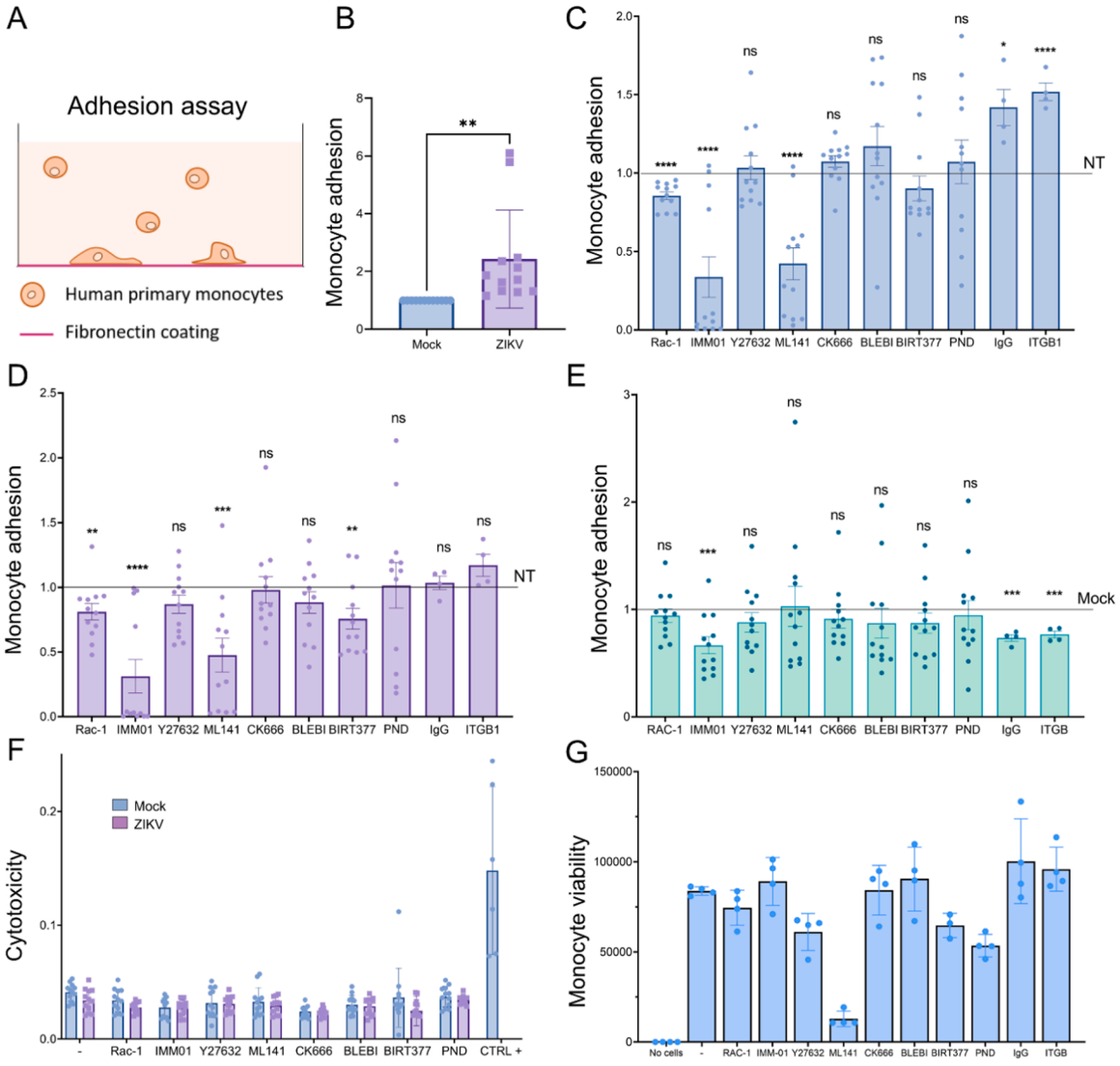

Fig. 1. Impact of ZIKV infection on the pharmacological inhibition of monocyte adhesion. (**A**) Representative scheme of an adhesion assay with a well coated with recombinant fibronectin and human primary monocytes added on top. (**B**) The bar graph represents the relative number of adherent monocytes on fibronectin, infected for 48 h with ZIKV or not (Mock). This assay was measure using CellTiter Glo. Each bar graph represents the pull of six healthy donors in duplicate and showing the mean ± SD from three individual experiments. (**C-D**) The bar graph represents the relative number of non-infected (**C**) or ZIKV-infected (**D**) monocytes adherent on fibronectin and treated with drugs targeting Rac1 (Rac1 inh, 50 μM), mDia (IMM-01, 30 μM), ROCK (Y-27632, 30 μM), Cdc42 (ML141, 50 μM), Arp2/3 (CK666, 30 μM), class 2 Myosins (Blebbistatin, 50 μM), LFA-1 (BIRT-377, 30 μM), FAK (PND, 1 μM) and neutralizing antibody against IgG (negative control) and integrin β1 (ITGB1/CD29). This assay was measured using CellTiter Glo. Each bar graph represents the pull of six healthy donors in duplicate and showing the mean ± SD from three individual experiments. (**E**) The bar graph represents the ratio of adherent ZIKV- infected monocytes compared to Mock-infected monocytes from the experiment in (**C**) and (**D**). (**F**) The bar graph represents the cytotoxicity in each experiment measured by LDH assay. The bar graph shows mean +/- SD from the monocytes obtained from 6 individual donors, performed in duplicates in three independent experiments. Unpaired student T-test p value < 0.05 (*), < 0.01 (**), < 0.005 (***), < 0.0001 (****); ns: non-significant. (G) The bar graph represents the monocytes viability measured by CellTiter Glo assay. The bar graph shows mean +/- SD from the monocytes performed in quadruplicate in one experiment.

impact of these Rho GTPase on virus-induced cell migration remains mostly unexplored.

2. Results

Our previous work highlighted that human primary monocytes exposed to ZIKV were over-expressing proteins involved in actin dynamics and FA (Ayala-Nunez et al., 2019). Human primary monocytes do not typically form FA (Kameritsch and Renkawitz, 2020) and we hence decided to further investigate what are the mechanisms underlying the impact of ZIKV on monocyte adhesion and migration. First, we validated our assay by comparing the ability of human primary monocytes to adhere on fibronectin upon exposure to ZIKV (Fig. 1A). We chose to focus on fibronectin adhesion as BBB-derived endothelial hCMEC/D3 cells exibit significant fibronectin coating on their apical side, and monocytes adhere more onto fibronectin than onto collagen (Suppl. Figure S1A-B). We confirmed that ZIKV-exposed monocytes adhere significantly more on fibronectin than their mock-infected counterparts (Fig. 1B). Next, we evaluated the impact of drugs targeting Rac1, mDia (IMM01), ROCK (Y27632), ML141 (Cdc42), Arp2/3 (CK666), class 2 Myosins (Bleb), LFA-1 (BIRT377), and focal adhesion kinase (FAK) PND-1186 (PND). We also used a neutralizing antibody targeting integrin b1 (ITGB1) as well as an isotype control (IgG). We found that targeting mDia and Cdc42 induced a significant decrease of monocyte adhesion in mock-exposed as well as ZIKV-exposed cells (Fig. 1C-D). The mock-exposed monocytes also showed increased adhesion properties upon treatment with IgG control and anti-ITGB1 antibodies (Fig. 1C), suggesting that antibody treatment may non-specifically increase monocyte adhesion. Differential analysis of the dataset showed that ZIKV-exposed monocytes were more dependent on mDia for adhesion than their mock-exposed counterpart (Fig. 1E). Antibody treatment also had a differential impact on ZIKV versus mock-exposed monocytes, although the lack of specificity of these conditions prevents interpretation. These treatments had no significant cytotoxicity on mock- or ZIKV-exposed monocytes using LDH assay, while CellTiter Glo assay showed decreased viability for the ML141 condition (Fig. 1F-G). Of note, the expression of CD16 and CD11b, two markers of monocytic polarization, were not significantly changed by the treatments (Suppl. Figure S2A-B)FA.

As collagen is present at the basal membrane of endothelial cells, we next evaluated the ability of monocytes to migrate through a collagen layer using 5-μm porous transwells pre-coated with type I collagen (in the absence of endothelium; Fig. 2A). The bottom chamber of the transwell corresponds to monocytes that successfully migrated through the collagen. Comparison of migration capacities of mock- versus ZIKV-exposed monocytes showed no statistically significant differences between the two conditions (Fig. 2B). However, most of the compounds tested had a significant impact on monocyte migration (Fig. 2C-D). Only the FAK inhibitor (PND) had no significant effect on monocyte migration, which can be explained by the mostly amoeboid nature of the migration of monocytes, which form immature FA (Kameritsch and Renkawitz, 2020). Differential analysis of ZIKV/mock-exposed monocyte migration did not reveal any significant difference (Fig. 2E), indicating that similar strategies are used by monocytes during migration through collagen, independently of their infection status.

The transmigration of monocytes through a BBB-like endothelial

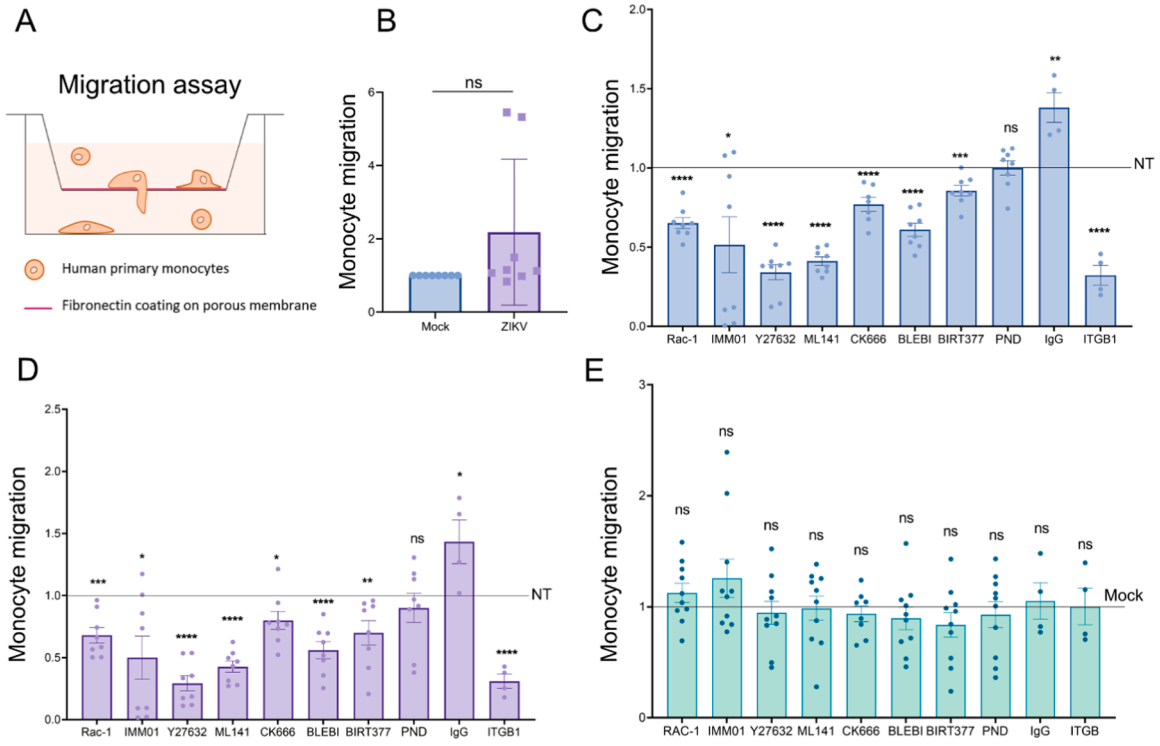

Fig. 2. Impact of ZIKV infection on the pharmacological inhibition of monocyte migration. (**A**) Representative scheme of a migration assay with a transwell coated with fibronectin and human primary monocytes added on top. (**B**) The bar graph represents the relative number of migrated monocytes harvested at the bottom of the well, infected with ZIKV for 48 h or not (Mock). This assay was measure using CellTiter Glo. Each bar graph represents the pull of four healthy donors in duplicate and showing the mean ± SD from three individual experiments. (**C-D**) The bar graph represents the relative number of non-exposed (**C**) or ZIKV-exposed (**D**) migrated monocytes and treated with molecules targeting Rac1 (Rac1 inh, 50 μM), mDia (IMM-01, 30 μM), ROCK (Y-27632, 30 μM), Cdc42 (ML141, 50 μM), Arp2/3 (CK666, 30 μM), class 2 Myosins (Blebbistatin, 50 μM), LFA-1 (BIRT-377, 30 μM), FAK (PND, 1 μM) and neutralizing antibody against IgG (negative control) and integrin β1 (ITGB1). This assay was measure using CellTiter Glo. Each bar graph represents the pool of four healthy donors in duplicate and showing the mean ± SD from three individual experiments. (**E**) The bar graph represents the ratio of migrated ZIKV-infected monocytes compared to Mock-infected monocytes from the experiment in (**C**) and (**D**). The bar graph shows mean +/- SD from monocytes obtained from four healthy donors, performed in duplicates in three independent experiments. Unpaired student T-test p value < 0.05 (*), < 0.01 (**), < 0.005 (***), < 0.0001 (****); ns: non-significant.

wall requires additional migratory properties, as monocytes need to squeeze through this endothelial fence. To study the impact of ZIKV on monocyte transmigration, BBB-derived endothelial hCMEC/D3 cells were seeded on 5-μm porous collagen-treated transwells and monocytes were allowed to transmigrate overnight in the presence of indicated compounds (Fig. 3A). As previously reported (Ayala-Nunez et al., 2019), we found that monocytes exposed to ZIKV transmigrated significantly more through endothelial cells than their non-exposed counterparts (Fig. 3B). All three Rho GTPase Rac1, ROCK and Cdc42 inhibitors significantly decreased monocyte transmigration in mock- and ZIKV-exposed monocytes (Fig. 3C-D). Although we cannot distinguish whether the effects of the inhibitors are due to their action on monocytes, endothelial cells or both, the impact of the inhibitors on the endothelium was evaluated by monitoring the distribution of VE-Cadherin in hCMEC/D3 cells. No visible perturbations of VE-Cadherin junctions on the endothelium were observed upon treatment with mDia, Arp2/3 and ROCK inhibitor, while Cdc42 inhibitor ML141 resulted in a disrupted endothelial monolayer (Suppl. Figure S3).

Differential analysis confirmed that ZIKV-exposed monocytes use Rho GTPases similarly to their mock-exposed counterparts (Fig. 3E). Interestingly, BIRT377, an inhibitor of LFA-1, did not impact mock-exposed monocyte transmigration (and actually tended to increase it) (Fig. 3C), consistent with previous work demonstrating that integrin-based adhesion is not required for rapid leukocyte migration (Lammermann et al., 2008). Strikingly however, ZIKV-exposed monocyte transmigration was significantly impaired by BIRT377, which was confirmed upon Mock/ZIKV differential analysis (Fig. 3D-E). This data highlighted that ZIKV-exposed monocytes, but not their mock-exposed counterparts, require functional LFA-1 integrins for efficient transmigration through the BBB-like endothelial layer.

Confocal microscopy of VE-cadherin and the polymerized actin cytoskeleton of hCMEC/D3 cells showed similar endothelial layer integrity regardless of BIRT377 treatment and/or the presence of ZIKV-exposed monocytes (Fig. 4A). Of note, the actin elements may have not been fully preserved by our fixation-permeabilization procedure, and cytoskeletal stabilization methods could be implemented to improve it, as previously shown (Mason et al., 2019). Based on the known mode of action of BIRT377, we confirmed that it significantly decreased monocyte adhesion onto ICAM-1 substrate, the LFA-1 ligand (Fig. 4B), as opposed to its absence of effect on monocyte adhesion to fibronectin shown in Fig. 1. Interestingly, the addition of BIRT377 to ZIKV-exposed monocytes during transmigration resulted in an accumulation of monocytes on top of the BBB-like endothelium (Fig. 4C-D), which express high levels of fibronectin as shown in Suppl. Figure S1. This data indicates that inhibition of LFA-1 does not prevent monocyte adhesion, but rather a downstream diapedesis process specific to ZIKV exposure.

3. Discussion

Flaviviridae represent an important health threat, showing rising number of cases in the past decade, most probably due to the spread of *Aedes* mosquitoes. ZIKV was first detected in Europe in 2013 (Tappe et al., 2014), and recurrently since then. While the infection is mostly asymptomatic in adults, the virus can cause discrete cognitive disorders (Mavigner et al., 2018; Raper et al., 2020) for which very little mechanistic insights exist as most of the focus has been placed on pre-birth

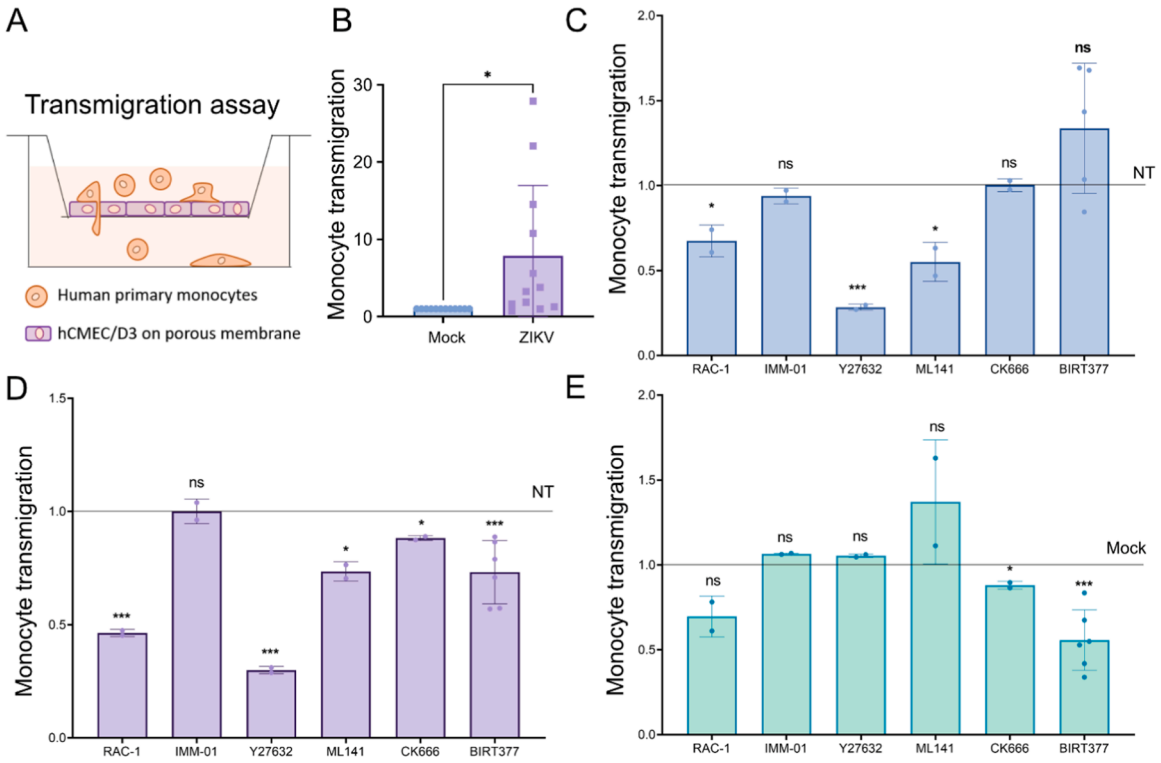

Fig. 3. Impact of ZIKV infection on the pharmacological inhibition of monocyte transmigration. (**A**) Representative scheme of a transmigration assay with a transwell coated with collagen and seeded with hCMEC/D3 endothelial cells forming permeable blood born barrier. Human primary monocytes were added on top. (**B**) The bar graph represents the relative number of transmigrated monocytes harvested at the bottom of the well, infected with ZIKV for 48 h or not (Mock). This assay was measure using CellTiter Glo. Each bar graph represents one healthy donor in duplicate. (**C-D**) The bar graph represents the relative number of non-infected (**C**) or ZIKV-infected (**D**) transmigrated monocytes and treated with drugs targeting Rac1 (Rac1 inh, 50 μM), mDia (IMM-01, 30 μM), ROCK (Y-27632, 30 μM), Cdc42 (ML141, 50 μM), Arp2/3 (CK666, 30 μM), LFA-1 (BIRT-377, 30 μM). This assay was measure using CellTiter Glo. (**E**) The bar graph represents the ratio of transmigrated ZIKV- infected monocytes compared to Mock-infected monocytes from the experiment in (**C**) and (**D**). The bar graph shows mean +/- SD from monocytes obtained from three healthy donor, performed in duplicates for the non-treated and the BIRT377 treated conditions. The other conditions were performed on one donor in duplicates. Unpaired student T-test p value < 0.05 (*), < 0.005 (***), ns: non-significant.

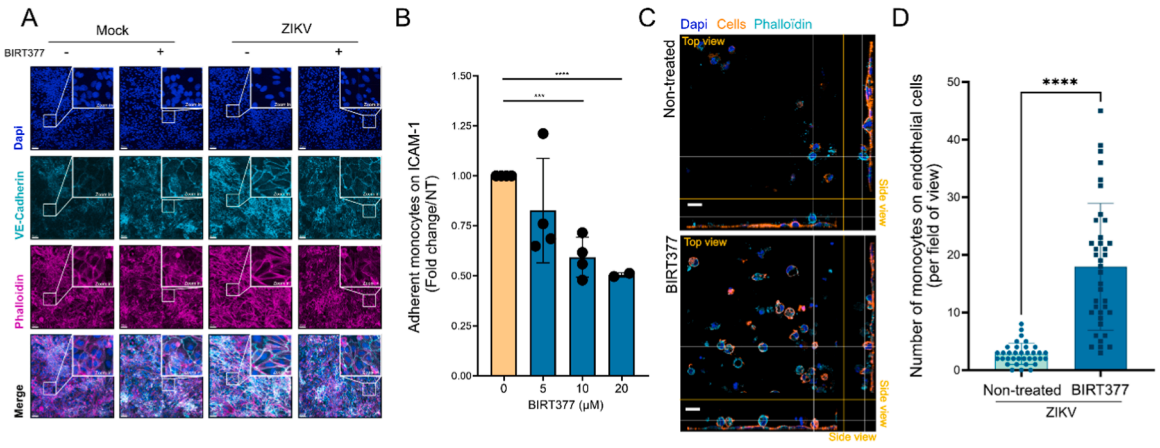

Fig. 4. Impact of BIRT377 on endothelial-monocyte interactions. (**A**) The micrograph represents the hCMEC-D3 monolayer incubated with mock-exposed of ZIKV-exposed monocytes in the presence or absence of 30 μM BIRT-377. The VE-cadherin staining is in cyan, the actin (phalloidin) in purple and the nuclei (DAPI) in blue. Scale bar: 50 μm. (**B**) The bar graph shows the mean +/- SD of adherent monocytes on ICAM-1 treated with BIRT377 (5 μM, 10 μM, or 20 μM) normalized to the non-treated condition (0 μM). Each bar represents data from two healthy donors performed in duplicates. The 20 μM condition was done on one healthy donor in duplicate. Unpaired student T-test p value < 0.001 (***) and < 0.0001 (****). (**C-D**) ZIKA-exposed monocytes were added on top of hCMEC/D3in the absence (**C**, upper panel), or presence (**C**, lower panel) of BIRT377. Actin (Phalloidin) is in Cyan and the monocytes are in orange. Scale bar: 20 μm. (**D**) Quantification of the number of adherent monocytes for each condition. The bar graph shows mean +/- SD from the monocytes obtained from 2 donors, performed in quadruplicates. Unpaired student T-test p value < 0.0001 (****).

neural defects. We have shown previously that ZIKV can reprogram monocytes to favor their transmigration through the BBB and disseminate in the CNS (Ayala-Nunez et al., 2019). This was due to increased adhesive properties associated to important cellular morphological rearrangements. Here, we used a non-exhaustive panel of pharmacological inhibitors based on the available literature and relevance with regards to ZIKV infection, to identify host factors specific for ZIKV-exposed monocyte transmigration.

The small Rho GTPases are known to play an important role during the transmigration of monocytes through endothelial cells (Wittchen et al., 2005). Here, we confirmed that monocyte adhesion, migration and transmigration require functionally active small Rho GTPases, regardless of the infection status of the monocyte. Inhibition of Cdc42 resulted in a profound inhibition of monocyte adhesion. Previous work has shown that Cdc42, but not Rac1 nor Myosin-II, is important for chemokine-driven trans-endothelial migration of CD4 T cells (Manes and Pober, 2013). Moreover, the cytoskeleton-associated protein WASP, a major Cdc42 effector, has been shown to play an important role during integrin-dependent leukocyte adhesion on endothelium during transmigration (Zhang et al., 2006). We show that the ROCK inhibitor significantly decreases migration and transmigration. Moreover, Myosin II, downstream of RhoA/ROCK signaling, also decreases monocyte migration. This is consistent with previous work showing that the RhoA/ROCK/Myosin-II axis is important for T cell transmigration through the control of actomyosin contractility (Heasman et al., 2010).

Our findings on the inhibition of small GTPases and actin-associated effectors were similar for both non-infected and ZIKV-exposed monocyte transmigration. However, we found that BIRT377 was the sole inhibitor that we tested to specifically impair ZIKV-exposed monocyte transmigration, while it did not affect mock-exposed monocyte transmigration. BIRT377 is an inhibitor of LFA-1 function, a heterodimeric receptor composed of CD11a and CD18 (Integrin β2). BIRT377 directly binds to and potently inhibits LFA-1 function by targeting the ligand interacting I-domain of the αL subunit of LFA-1 (Kelly et al., 1999; Shimaoka et al., 2002; Last-Barney et al., 2001). ICAM-1/LFA-1 interactions through the I-domain is involved in immune cell adhesion to endothelium (Jun et al., 2001; Shaw et al., 2004). We show that upon treatment with BIRT377, ZIKV-exposed monocytes transmigrate less compared to non-treated counterparts. Furthermore, we show that CD11a was significantly upregulated at the surface of monocytes exposed to ZIKV and that CD18 also tended to be overexpressed, although it did not reach significance (Ayala-Nunez et al., 2019). This result suggests that LFA-1 is particularly important for ZIKV-induced monocyte transmigration. Although this interaction is important for monocyte-to-endothelium adhesion, we observed that the BIRT377-treated monocytes adhered significantly more on the endothelium (but not on fibronectin alone), suggesting that the inhibition of ZIKV-induced monocyte transmigration by BIRT377 does not occur at the adhesion step but downstream in the process. The apparent increase of adhesion of ZIKV-exposed monocytes upon BIRT377 treatment would hence come from the inefficient transmigration step, blocking the monocytes on top of the endothelial monolayer. Of note, experiments of downregulation of the LFA-1 complex at the surface of monocytes will be required to ascertain whether BIRT377 exerts its anti-transmigratory properties by specifically targeting LFA-1, or through indirect mechanisms that remain to be identified.

Although LFA-1 is most known for its adhesion properties, it has also been shown to interact with JAM-A through its I-domain, the target domain of BIRT377. JAM-A is a tight junction-associated protein interacting in a homophilic manner that is involved in the regulation of leukocyte transmigration (Ostermann et al., 2002). In the presence of transmigrating leukocytes, the LFA-1 protein at the surface of the immune cell will act as a competitor of JAM-A/JAM-A interactions on the endothelium, forcing the LFA-1/JAM-A interaction to favor the local unzipping of the tight junctions and let the immune cell cross the endothelial monolayer (Wojcikiewicz et al., 2009). In contrast, JAM-A does not participate in neutrophil transmigration, while LFA-1/ICAM-1 interactions are important (Shaw et al., 2004). In our case, we could hypothesize that monocytes exposed to ZIKV exhibit enhanced transmigration properties due to increased LFA-1 surface expression levels (Ayala-Nunez et al., 2019), favoring the interactions between monocytic LFA-1 with endothelial JAM-A, and thus increasing transmigration efficiency compared to non-exposed monocytes. Treatment with BIRT377 would prevent transmigration, with a more significant effect on ZIKV-exposed monocytes as they express higher levels of LFA-1.

An early study proposed that LFA-1 plays a role in crawling and subsequent transmigration of monocytes only upon pretreatment with IL-1β or TNF (Schenkel et al., 2004). This observation suggests that ZIKV might activate monocytes and confer LFA-1-dependent

pro-transmigratory properties to favor the LFA-1/JAM-1 interaction and diapedesis process. Further investigations will be needed to determine whether ZIKV induces pro-inflammatory cytokine release. Moreover, it remains to be established whether the levels of LFA-1/JAM-1 proteins are modulated upon transmigration of ZIKV-exposed monocytes. Indeed, we have previously shown that CD11a and CD18 were upregulated at the surface of monocytes exposed to ZIKV (Ayala-Nunez et al., 2019). Thus, one can hypothesize that ZIKV-exposed monocytes crawl and transmigrate more through endothelia because they use an LFA-1-dependent migration strategy, which as a consequence, would make them more susceptible to BIRT377 treatment.

Finally, BIRT377 has previously been used to reverse neuropathic effects in rats, reducing immune infiltration to the CNS (Noor et al., 2020). Preventing viral and immune neuroinvasion represents an attractive strategy to counteract viro-induced neurological disorders (Gaudin et al., 2022). Here, we show that BIRT377 specifically acts on ZIKV-exposed cells, a targeted approach that could be used to treat ZIKV-induced neurological disorders and potentially other viral neuroinfections.

3.1. Material & methods

3.1.1. Reagents

The following antibodies and dye were used for immunofluorescence in this study: polyclonal goat anti VE-Cadherin (1/100, R&D Systems, #AF938), Phalloidin CF-633 (1/100, Biotium, #00046), Dapi Nuclear Counterstain (Pierce), CellTrace Yellow (Invitrogen), polyclonal sheep anti Fibronectin (1/100, Biorad, #VPA00045). For flow cytometry, the following antibody were used: REAfinity anti-human CD16 antibody coupled to APC (1/50, Miltenyi Biotech, #130-113-389) and REAfinity anti-human CD11b coupled to APC (1/50, Miltenyi Biotech, # 130-110-556). For adhesion and migration inhibition assay, the Rat monoclonal anti-CD29 antibody (BD Bioscience, Clone 9EG7, #553715) and the Rat IgG2b K isotype control (Invitrogen, 16-4031-81) were used at final concentration of 0.16 mg/mL.

Rac-1 Inhibitor II (Calbiochem, #553512) stock solution was resuspended at 100 mM in DMSO, IMM-01 (Sigma Aldrich, #SML1064) at 10 mg/mL in DMSO, Y-27632 Dihydrochloride 5 (Sigma Aldrich, # Y0503) at 10 mM in DMSO, ML141 (Tocris, #4266) at 10 mM in DMSO, CK666 (Sigma Aldrich, #SML0006) at 30 mM in DMSO, Blebbistatin (Sigma Aldrich, #203389) at 50 mM in DMSO, BIRT377 (Tocris, #4776) at 50 mM in DMSO, PND-1186 (Tocris, #6891) at 100 mM in DMSO.

3.2. Cells

Human primary monocytes were isolated from healthy donor coming from EFS Montpellier. All donors signed informed consent allowing the use of their blood for research purposes. Briefly, PBMCs were isolated from the blood of donor using a Ficoll density gradient (GE Healthcare) and primary monocytes were positively selected with $CD14^+$ microbeads and magnetic columns (Miltenyi Biotec). For experiment, the cells were cultured into round-bottom tissue culture-treated 96-well plates in RPMI 1640 (Gibco) media supplemented with 2 % FBS (Dutscher) and 1 % Penicillin–Streptomycin (Gibco).

The human Cerebellar Microvascular Endothelial Cells D3 (hCMEC/D3) cells (provided by S. Bourdoulous, Institut Cochin, France) were cultured in EndoGRO-MV Complete Culture Media (Millipore) supplemented with 1 ng/mL bFGF (Sigma) and 1 % Penicillin–Streptomycin (Gibco). When plated, the well was coated with rat collagen-I (R&D Systems) and the hCMEC/D3 cells were then cultured the media was supplemented with Lithium Chloride (10 mM) and Resveratrol (10 μM).

3.3. Virus and infection

The ZIKV FLR strain used in this study was obtained from BEI Resources, NIAID, NIH (NR-50183). The strain was isolated in December 2015 from the blood of an infected patient from Colombia. The virus was grown on Vero cells for 72 h then harvested. Cell debris were removed by centrifugation at 2000×*g* for 5 min, and aliquots stored at −80 °C. Viral titer (PFUs/mL) was determined on Vero by plaque assay. All experiments involving infectious ZIKV were performed in a BSL-3 facility.

Monocytes infection with ZIKV was performed by inoculating ZIKV at a multiplicity of infection (MOI) of 1 (from the titer calculated on Vero) in RPMI 1640 (Gibco) media supplemented with 2 % FBS (Dutscher) and 1 % Penicillin–Streptomycin (Gibco). The ZIKV-exposed monocytes were incubated for 48 h before use in assays. In all the experiments, "Mock" corresponds to the supernatant of Vero cells processed in the same way as for ZIKV production.

3.4. Cell viability and cytotoxicity

Cytotoxicity was measured using the CyQUANT LDH Cytotoxicity Assay Kit (Invitrogen) and performed according to the manufacturer's instructions. Briefly, supernatant was harvested and incubated in 96-well plate with the LDH substrate for 30 min at RT. The Stop Solution was added to each sample and the absorbance was measured with a microplate reader (TECAN Infinite M Plex).

Cell viability was measured using the CellTiter-Glo Luminescent Cell Viability Assay (Promega) and the experiment was performed according to the manufacturer's instructions. Briefly, cells were resuspended in culture medium and incubate with CellTiter-Glo Reagent for 10 min at RT. The luminescence signal was measured with a microplate reader (TECAN Infinite M Plex).

3.5. Adhesion assay

Adhesion assay were performed on with 96-well plates flat bottom coated with 5 $\mu g/cm^2$ of human fibronectin (R&D Systems), 150 μg/mL of collagen, type I solution from rat tail (Sigma-Aldrich), or 12.5 μg/mL of recombinant Human ICAM-1/CD54 (R&D Systems) for 1 h at RT. Primary monocytes were added on the coated substrate and incubated for 3 h at 37 °C and 5 % CO_2 to let the cells adhere. Then the wells were washed three times and the adherent monocytes were prepared for CellTiter-Glo Luminescent Cell Viability assay (Promega), according to the manufacturer instructions. The assay gives a sense of cell number, as estimated through ATP measurement.

3.6. Migration assay

Migration assay was performed on hanging 96 well plate cell culture inserts (PET, 5-μm pores, Millipore) coated with 5 $\mu g/cm^2$ of human fibronectin (R&D Systems). Primary monocytes were added on top of the insert and let over-night at 37 °C and 5 % CO_2. The bottom chamber was replaced with RPMI 2 % FBS supplemented with 200 ng/mL of MCP-1 (Miltenyi Biotech). Cells of the bottom chamber were harvested and lysed with CellTiter-Glo Luminescent Cell Viability Assay.

3.7. Transmigration assay

Transmigration was done on cell culture inserts (PET, 5-μm pores, Millipore) coated with rat collagen type 1 (Sigma). The hCMEC/D3 were then seeded on the transwell for 7 days to reach impermeability properties. Two hundred thousand monocytes (infected or not) were treated for 30 min with the drugs and add on top of the transwell to let the transmigration occur over night at 37 °C and 5 % CO_2. The bottom chamber was replaced with RPMI 2 % FBS supplemented with 200 ng/mL of MCP-1 (Miltenyi Biotech). Cells of the bottom chamber were harvested and lysed with CellTiter-Glo Luminescent Cell Viability Assay (Promega).

3.8. Fluorescence confocal microscopy

Cells were cultured in 96 square well plate glass bottoms. After transmigration assay, cells were washed once with phosphate buffered saline (PBS) and fixed with 4 % paraformaldehyde (PFA) for 20 min at room temperature (RT). Samples were then permeabilized for 20 min with permeabilization buffer (0.5 % BSA, 0.1 % Triton in PBS). All subsequent steps were performed in permeabilization buffer. Samples were labeled with primary antibody for 3 h at RT, washed twice and labeled with appropriate secondary antibodies and dye for 45 min. Cells were washed twice with the permeabilization buffer and imaged in the same buffer. Image acquisition was performed on a spinning-disk confocal microscope (Dragonfly, Oxford Instruments). The ultrasensitive 1024 × 1024 EMCCD camera (iXon Life 888, Andor) used has four laser lines (405, 488, 561, and 637 nm. A 40x, NA 1.3 oil-immersion was used to look at BBB integrity whereas 60x, NA 1.15 (Nikon) oil-immersion long-distance objective was used for counting monocytes on the monolayer. Images were processed using FiJi (ImageJ) and Bitplane Imaris x64 (Oxford Instruments) version 9.2 and 9.7.

3.9. Flow cytometry

Human primary monocytes were fixed in 4 % PFA and washed in PBS. Samples were blocked with 10 % FBS in PBS and 1:5 FcR Blocking Reagent (Miltenyi Biotech) and were stained with primary conjugated antibodies at 4 °C for 1 h. Cells were washed 2x with PBS. Samples were acquired with NovoCyte Flow Cytometry System (ACEA Biosciences). Data was analyzed using FlowJo (LLC) v10.2.

CRediT authorship contribution statement

Emma Partiot: Writing – review & editing, Visualization, Validation, Methodology, Investigation, Formal analysis, Data curation. **Raphael Gaudin:** Writing – review & editing, Writing – original draft, Visualization, Supervision, Resources, Project administration, Methodology, Investigation, Funding acquisition, Formal analysis, Conceptualization. **Diana Brychka:** Investigation, Methodology, Writing – review & editing.

Declaration of Competing Interest

The authors declare that they have no known competing financial interests or personal relationships that could have appeared to influence the work reported in this paper.

Data availability

Data will be made available on request.

Acknowledgments

We thank Diane Bégarie for her help in the experiments. The following reagent was obtained through BEI Resources, NIAID, NIH: Zika Virus, FLR, NR-50183. Funding: we thank the Agence Nationale de la Recherche ANR-20-CE15-0019-01 to RG, the CBS2 Montpellier doctoral school to EP, and Sidaction to DB.

Conflict of interest

The authors declare no conflict of interest.

Appendix A. Supporting information

Supplementary data associated with this article can be found in the online version at doi:10.1016/j.ejcb.2024.151453.

References

Aid, M., et al., 2017. Zika virus persistence in the central nervous system and lymph nodes of rhesus monkeys. Cell 169, 610–620 https://doi.org:10.1016/j.cell.2017.04.008.
Ayala-Nunez, N.V., et al., 2019. Zika virus enhances monocyte adhesion and transmigration favoring viral dissemination to neural cells. Nat. Commun. 10, 4430 https://doi.org:10.1038/s41467-019-12408-x.
Baud, D., Gubler, D.J., Schaub, B., Lanteri, M.C., Musso, D., 2017. An update on Zika virus infection. Lancet https://doi.org:10.1016/S0140-6736(17)31450-2.
Bhatnagar, J., et al., 2017. Zika virus RNA replication and persistence in brain and placental tissue. Emerg. Infect. Dis. 23, 405–414 https://doi.org:10.3201/eid2303.161499.
Gaudin, R., Brychka, D., Sips, G.J., Ayala-Nunez, V., 2022. Targeting tight junctions to fight against viral neuroinvasion. Trends Mol. Med. 28, 12–24 https://doi.org:10.1016/j.molmed.2021.10.007.
Hall, A., 1998. Rho GTPases and the actin cytoskeleton. Science 279, 509–514 https://doi.org:10.1126/science.279.5350.509.
Heasman, S.J., Carlin, L.M., Cox, S., Ng, T., Ridley, A.J., 2010. Coordinated RhoA signaling at the leading edge and uropod is required for T cell transendothelial migration. J. Cell Biol. 190, 553–563 https://doi.org:10.1083/jcb.201002067.
Hirsch, A.J., et al., 2017. Zika Virus infection of rhesus macaques leads to viral persistence in multiple tissues. PLoS Pathog. 13, e1006219 https://doi.org:10.1371/journal.ppat.1006219.
Jun, C.D., Shimaoka, M., Carman, C.V., Takagi, J., Springer, T.A., 2001. Dimerization and the effectiveness of ICAM-1 in mediating LFA-1-dependent adhesion. Proc. Natl. Acad. Sci. USA 98, 6830–6835 https://doi.org:10.1073/pnas.121186998.
Kameritsch, P., Renkawitz, J., 2020. Principles of leukocyte migration strategies. Trends Cell Biol. 30, 818–832 https://doi.org:10.1016/j.tcb.2020.06.007.
Kelly, T.A., et al., 1999. Cutting edge: a small molecule antagonist of LFA-1-mediated cell adhesion. J. Immunol. 163, 5173–5177.
Lammermann, T., et al., 2008. Rapid leukocyte migration by integrin-independent flowing and squeezing. Nature 453, 51–55 https://doi.org:10.1038/nature06887.
Last-Barney, K., et al., 2001. Binding site elucidation of hydantoin-based antagonists of LFA-1 using multidisciplinary technologies: evidence for the allosteric inhibition of a protein–protein interaction. J. Am. Chem. Soc. 123, 5643–5650 https://doi.org:10.1021/ja0104249.
Laval, K., Favoreel, H.W., Poelaert, K.C., Van Cleemput, J., Nauwynck, H.J., 2015. Equine Herpesvirus Type 1 enhances viral replication in CD172a+ monocytic cells upon adhesion to endothelial cells. J. Virol. 89, 10912–10923 https://doi.org:10.1128/JVI.01589-15.
Lessler, J., et al., 2016. Assessing the global threat from Zika virus. Science 353, aaf8160 https://doi.org:10.1126/science.aaf8160.
Li, H., et al., 2016a. Zika Virus Infects Neural Progenitors in the Adult Mouse Brain and Alters Proliferation. Cell Stem Cell 19, 593–598 https://doi.org:10.1016/j.stem.2016.08.005.
Li, Z.L., Liang, X., Li, H.C., Wang, Z.M., Chong, T., 2016b. Dendritic cells serve as a "Trojan horse" for oncolytic adenovirus delivery in the treatment of mouse prostate cancer. Acta Pharm. Sin. 37, 1121–1128 https://doi.org:10.1038/aps.2016.59.
Li, H., Saucedo-Cuevas, L., Shresta, S., Gleeson, J.G., 2016a. The neurobiology of Zika virus. Neuron 92, 949–958 https://doi.org:10.1016/j.neuron.2016.11.031.
Manes, T.D., Pober, J.S., 2013. TCR-driven transendothelial migration of human effector memory CD4 T cells involves Vav, Rac, and myosin IIA. J. Immunol. 190, 3079–3088 https://doi.org:10.4049/jimmunol.1201817.
Mason, D.E., et al., 2019. YAP and TAZ limit cytoskeletal and focal adhesion maturation to enable persistent cell motility. J. Cell Biol. 218, 1369–1389 https://doi.org:10.1083/jcb.201806065.
Mavigner, M., et al., 2018. Postnatal Zika virus infection is associated with persistent abnormalities in brain structure, function, and behavior in infant macaques. Sci. Transl. Med. 10 https://doi.org:10.1126/scitranslmed.aao6975.
Noor, S., et al., 2020. The LFA-1 antagonist BIRT377 reverses neuropathic pain in prenatal alcohol-exposed female rats via actions on peripheral and central neuroimmune function in discrete pain-relevant tissue regions. Brain Behav. Immun. 87, 339–358 https://doi.org:10.1016/j.bbi.2020.01.002.
Ostermann, G., Weber, K.S., Zernecke, A., Schroder, A., Weber, C., 2002. JAM-1 is a ligand of the beta(2) integrin LFA-1 involved in transendothelial migration of leukocytes. Nat. Immunol. 3, 151–158 https://doi.org:10.1038/ni755.
Paul, A.M., et al., 2017. Osteopontin facilitates West Nile virus neuroinvasion via neutrophil "Trojan horse" transport. Sci. Rep. 7, 4722 https://doi.org:10.1038/s41598-017-04839-7.
Peluso, R., Haase, A., Stowring, L., Edwards, M., Ventura, P., 1985. A Trojan Horse mechanism for the spread of visna virus in monocytes. Virology 147, 231–236.
Pierson, T.C., Diamond, M.S., 2018. The emergence of Zika virus and its new clinical syndromes. Nature 560, 573–581 https://doi.org:10.1038/s41586-018-0446-y.
Raper, J., et al., 2020. Long-term alterations in brain and behavior after postnatal Zika virus infection in infant macaques. Nat. Commun. 11, 2534 https://doi.org:10.1038/s41467-020-16320-7.
Schenkel, A.R., Mamdouh, Z., Muller, W.A., 2004. Locomotion of monocytes on endothelium is a critical step during extravasation. Nat. Immunol. 5, 393–400 https://doi.org:10.1038/ni1051.
Shaw, S.K., et al., 2004. Coordinated redistribution of leukocyte LFA-1 and endothelial cell ICAM-1 accompany neutrophil transmigration. J. Exp. Med. 200, 1571–1580 https://doi.org:10.1084/jem.20040965.
Shimaoka, M., Takagi, J., Springer, T.A., 2002. Conformational regulation of integrin structure and function. Annu. Rev. Biophys. Biomol. Struct. 31, 485–516 https://doi.org:10.1146/annurev.biophys.31.101101.140922.

Tang, H., et al., 2016. Zika virus infects human cortical neural progenitors and attenuates their growth. Cell Stem Cell 18, 587–590 https://doi.org:10.1016/j.stem.2016.02.016.
Tappe, D., et al., 2014. First case of laboratory-confirmed Zika virus infection imported into Europe, November 2013. Eur. Surveill. 19.
Tiong, V., Shu, M.H., Wong, W.F., AbuBakar, S., Chang, L.Y., 2018. Nipah virus infection of immature dendritic cells increases its transendothelial migration across human brain microvascular endothelial cells. Front Microbiol 9, 2747 https://doi.org:10.3389/fmicb.2018.02747.
Van den Broeke, C., Jacob, T., Favoreel, H.W., 2014. Rho'ing in and out of cells: viral interactions with Rho GTPase signaling. Small GTPases 5, e28318 https://doi.org:10.4161/sgtp.28318.
Vicente-Manzanares, M., Choi, C.K., Horwitz, A.R., 2009. Integrins in cell migration–the actin connection. J. Cell Sci. 122, 199–206 https://doi.org:10.1242/jcs.018564.
Weber, C., Fraemohs, L., Dejana, E., 2007. The role of junctional adhesion molecules in vascular inflammation. Nat. Rev. Immunol. 7, 467–477 https://doi.org:10.1038/nri2096.
Wittchen, E.S., van Buul, J.D., Burridge, K., Worthylake, R.A., 2005. Trading spaces: Rap, Rac, and Rho as architects of transendothelial migration. Curr. Opin. Hematol. 12, 14–21 https://doi.org:10.1097/01.moh.0000147892.83713.a7.
Wojcikiewicz, E.P., et al., 2009. LFA-1 binding destabilizes the JAM-A homophilic interaction during leukocyte transmigration. Biophys. J. 96, 285–293 https://doi.org:10.1529/biophysj.108.135491.
Yockey, L.J., et al., 2016. Vaginal exposure to Zika virus during pregnancy leads to fetal brain infection. Cell 166, 1247–1256 https://doi.org:10.1016/j.cell.2016.08.004.
Zhang, H., et al., 2006. Impaired integrin-dependent function in Wiskott-Aldrich syndrome protein-deficient murine and human neutrophils. Immunity 25, 285–295 https://doi.org:10.1016/j.immuni.2006.06.014.